Proton-neutron force and proton single-particle strength in Sc, F, and Li isotopes

Pawan Kumar,* Shahariar Sarkar, Pushpendra P. Singh, and P. K. Raina
Department of Physics, Indian Institute of Technology Ropar, Rupnagar, Punjab-140001, India

(Received 23 May 2019; published 21 August 2019)

In the present work, the effect of proton-neutron interaction and its different components, i.e., central, spin-orbit, and tensor force, on proton shell-structure of odd-A Sc, F, and Li isotopes is studied within the nuclear shell model framework. It has been observed that the central force possesses strong-orbital node (nl) and weak-spin (j) dependency, and plays a key role in producing changes in proton shell-structure. The integrated effect of proton shell-structure and proton single-particle strength in building the level structure of ^{49,53,55}Sc, ^{23,25}F, and ^{9}Li isotopes are also discussed. Proton single-particle strength in the level structure of above-mentioned nuclei is studied using proton-transfer spectroscopic factors. It has been particularly discerned that the low energy of the $\frac{3}{2}^{-}_{1}$ state of ^{55}Sc is caused by the weakening of the $N = 34$ semimagic gap, the high energy of the $\frac{1}{2}^{+}_{1}$ state of ^{23}F is originated from an increase in the energy gap between orbitals $\pi 1s_{1/2}$ and $\pi 0d_{5/2}$ at $N = 14$, and the high energy of the $\frac{1}{2}^{-}_{1}$ state of ^{9}Li is originated from the large energy gap between $\pi 0p_{1/2}$ and $\pi 0p_{3/2}$ orbitals which remained nearly constant from ^{5}Li to ^{9}Li.

DOI: 10.1103/PhysRevC.100.024328

I. INTRODUCTION

At the femtometer scale, properties of many-body microscopic system (*atomic nucleus*) depend on the interaction among its constituents (*protons and neutrons*). In the pioneering work of Mayer [1], it was shown that the average nucleon interaction, which can be treated by spherical mean-field, along with the spin-orbit interaction gives rise to the shell-like structure in atomic nuclei. The shell structure is also seen in atoms, however, it is considerably different from the shell structure of atomic nuclei. In atoms, it remains as a universal property, whereas, in atomic nuclei, it changes considerably depending on neutron to proton number asymmetry [2].

The change in shell structure in atomic nuclei, often called shell evolution, is one of the important topics of modern nuclear physics. With the availability of radioactive ion beams and state-of-the-art detectors, the nuclear structure of very short-lived neutron-rich nuclei far away from the line of β stability has been extensively explored for more than two decades. The observations such as (i) the appearance of new shell gaps at $N = 14$, 16, 32, and 34 [3–7], (ii) the disappearance of traditional $N = 8$ shell gap for $Z = 2$–4 nuclei [8–11], $N = 20$ shell gap for $Z = 8$–12 nuclei [12–18], and $N = 28$ shell gap for $Z < 16$ nuclei [19,20], and (iii) the change in conventional ordering of single-particle orbitals in Ca, Cu, and Sb isotopes [7,21], are a few examples which show shell evolution. These observations, in turn, limit the predictive power of theoretical nuclear many-body models, and present challenges for a theoretician to precisely understand the causes of shell evolution. A detailed study on shell evolution is also important from the astrophysics point of interest as reliable predictions are required to predict shell structure in very neutron-rich nuclei, particularly along r-path nucleosynthesis.

In order to uncover the origin of shell evolution, many theoretical efforts have been made in the past, the role of nucleon-nucleon (NN) interaction has been discussed in particular. In the nuclear shell model framework, Otsuka and his collaborators have unveiled that the spin-isospin part of tensor force $f(r)[Y^2 \cdot (\sigma_1 \otimes \sigma_2)^2]^0$ of the $\pi + \rho$ meson exchange potential acting between the proton and neutron is a predominant source of changing the single-particle energy gaps [22]. Its robust effect on the variation of single-particle energy gaps in the series of isotopes and isotones has been studied in Refs. [22,23]. Due to its success in explaining the shell evolution, it has been explicitly implemented into the mean-field calculations [24–27]. Furthermore, this force shows renormalization persistency against the microscopic approaches followed to incorporate short-range repulsion of the NN interaction and in-medium effects [28].

In practice, NN interactions used in shell model studies are phenomenological. Therefore, a more rigorous method to determine the role of effective shell model interaction and its different components, i.e., central, spin-orbit, and tensor force, in the shell evolution has been put forward in studies [29,30]. Mainly, the proton-neutron part of the interaction has been explored. In Ref. [29], the contribution of central and tensor forces has been found important for the evolution of $N = 20$ and 28 shell gaps, whereas in Ref. [30], the contribution of central force has been found crucial for the evolution of the $N = 8$ shell gap. These studies are based on spin-tensor decomposition [31,32] that allows to decompose the effective shell model interaction into its different components. Furthermore, it has been shown to be a useful tool to determine why realistic microscopic interactions fail to describe shell evolution in neutron-rich nuclei [29], and also to unfold the resemblance and the discrepancies between microscopic and phenomenological shell model interactions, if any [33].

*pawan.kumar@iitrpr.ac.in

In this article, we intend to examine the effect of proton-neutron interaction on the proton shell structure of odd-A isotopes, having one proton above a closed proton shell, e.g., Sc, F, and Li isotopes. Recently, new intriguing experimental data on the spectra of very neutron-rich Sc and F isotopes have been reported [34–39], which hint a strong influence of proton-neutron interaction on the variation in protons single-particle energy gaps. For instance, in a naive picture, the low excited $\frac{3}{2}^-_1$ state of ^{55}Sc indicates the disappearance of the $Z = 28$ shell gap, whereas, the high excited $\frac{1}{2}^+_1$ state of ^{23}F connotes a large single-particle energy between $\pi 0d_{5/2}$ and $\pi 1s_{1/2}$ orbitals.

In this work, calculations for Sc, F, and Li isotopes have been carried out in $0f1p$, $0d1s$, and $0p$ shells, respectively, in the nuclear shell model framework. As calculations are possible within a single-oscillator shell, we have employed spin-tensor decomposition in order to gain a better understanding of the role of proton-neutron central, spin-orbit, and tensor forces in producing the proton shell evolution. We have also calculated proton single-particle strength in the ground state and excited states of ^{49,53,55}Sc and ^{23,25}F and ^{9}Li isotopes and presented the integrated effect of proton single-particle energy gaps and proton single-particle strength in building their level structure. Furthermore, we have demonstrated spin-tensor decomposition as a useful method for improving the discrepancies present in the effective interaction, and is shown for the $0p$-shell interaction.

This article is organized as follows. In Sec. II, the theoretical framework is given which contains compact derivation of single-particle energies for proton-$0f1p$, $0d1s$, and $0p$ orbitals of Sc, F, and Li isotopes, respectively, and spin-tensor decomposition. In Sec. III A, the contribution of the proton-neutron interaction and its different components in the proton shell evolution in the Sc, F, and Li isotopic chain is summarized. The integrated effect of proton single-particle energy gaps and proton single-particle strength in building the level structure of ^{49,53,55}Sc, ^{23,25}F, and ^{9}Li isotopes are discussed in Sec. III B. The summary of this work is presented in Sec. IV.

II. THEORETICAL FRAMEWORK

A few methods have been proposed to calculate the single-particle energy, also called effective single-particle energy (ESPE), of an orbital in the nuclear shell model framework [29,30,33,40]. In the present work, the ESPEs of proton orbitals for odd-A Sc, F, and Li isotopes are determined with respect to even-$(A-1)$ Ca, O, and He isotopes, respectively, which is considered a zeroth-order approximation [41,42]. They are calculated using the monopole Hamiltonian of the shell-model Hamiltonian $\hat{H}$ [43–45]. In the proton-neutron formalism, the monopole Hamiltonian is given as

$$\hat{H}_m = \sum_i \varepsilon_{\pi_i}\hat{n}_{\pi_i} + \sum_i \varepsilon_{\nu_i}\hat{n}_{\nu_i} + \sum_{i\leqslant j}\frac{\hat{n}_{\pi_i}(\hat{n}_{\pi_j}-\delta_{ij})}{1+\delta_{ij}}\bar{V}^{\pi\pi}_{ij} + \sum_{i\leqslant j}\frac{\hat{n}_{\nu_i}(\hat{n}_{\nu_j}-\delta_{ij})}{1+\delta_{ij}}\bar{V}^{\nu\nu}_{ij} + \sum_{ij}\hat{n}_{\pi_i}\hat{n}_{\nu_j}\bar{V}^{\pi\nu}_{ij}, \quad (1)$$

where $\hat{n}_{\rho_i}$ is number operator for particle type ρ and orbital i. The index i consists of all quantum numbers (n, l, and j) to define an orbital, and ε is unperturbed single-particle energy of an orbital. $\bar{V}$ is total angular momentum (J) averaged NN matrix elements, which is expressed as

$$\bar{V}^{\rho\rho'}_{ij} = \frac{\sum_J (2J+1)(1+(-1)^J\delta_{\rho\rho'}\delta_{ij})V^{\rho\rho'}_{ij;J}}{(2i+1)(2j+1-\delta_{\rho\rho'}\delta_{ij})}, \quad (2)$$

where summation runs only over the Pauli principle allowed J values.

For the calculations of Sc isotopes, GXPF1B interaction [46] with modifications of $\bar{V}^{T=1}_{p_{3/2}f_{5/2}}$ by -0.15 MeV [7], and $\bar{V}^{T=0}_{f_{7/2}p_{3/2}}$ by $+0.14$ MeV is considered. We have modified the latter matrix element to better reproduce the excitation energy of the $\frac{3}{2}^-_1$ state of ^{49}Sc. This new effective interaction, hereafter, is denoted as the GX1N interaction. For the calculations of F isotopes, the universal-sd-B (USDB) interaction [47] is considered.

Using Eq. (1), the deduced expression of ESPE of a proton orbital j' in Sc and F isotopes, under the normal filling of neutron orbitals, is given as [41]

$$\varepsilon'^{\pi}_{j'}(A) = \varepsilon^{\pi}_{j'} + \sum_{i\leqslant j} n^{\nu}_i \left(\frac{n^{\nu}_j - \delta_{ij}}{1+\delta_{ij}}\right)\left(\bar{V}^{\nu\nu}_{ij}(A) - \bar{V}^{\nu\nu}_{ij}(A-1)\right) + \sum_i n^{\nu}_i \bar{V}^{\nu\pi}_{ij'}(A). \quad (3)$$

In the above equation, indices i and j run over the filled valance neutron orbitals. The occurrence of the first summation term in the above equation is purely a consequence of atomic mass dependency of the employed shell model interactions, which does not allow to completely cancel the ν-ν interaction components when taking the difference of binding energies (the eigenvalues of the monopole Hamiltonian) of Sc and Ca isotopes, and F and O isotopes. The two-body matrix elements of GX1N and USDB interactions are scaled by mass correction factors $(42/A)^{0.3}$ and $(18/A)^{0.3}$, respectively.

In the $0p$ shell for Li isotopes, we consider CK(8-16) [48] and CKHeN interactions. CKHeN interaction is a hybrid interaction constructed in this work. Details of this interaction are discussed later in the article. Both of these interactions are independent of the mass correction factor, therefore, the first summation from Eq. (3) is removed. The expression of ESPE of a proton orbital in Li isotopes is given as

$$\varepsilon'^{\pi}_{j'} = \varepsilon^{\pi}_{j'} + \sum_i n^{\nu}_i \bar{V}^{\nu\pi}_{ij'}. \quad (4)$$

In order to get an insight into the contribution of different components of proton-neutron interaction to produce variation in proton single-particle energy gaps, we have decomposed the employed shell model interactions using spin-tensor decomposition.

Spin-tensor decomposition: The interaction between two nucleons can be written as the linear sum of scalar product of configuration space operator Q and spin space operator S of

rank k [31,32],

$$V = \sum_{k=0}^{2} V(k) = \sum_{k=0}^{2} Q^k \cdot S^k, \tag{5}$$

where rank $k = 0$, 1, and 2 represent central, spin-orbit, and tensor force, respectively. Using the LS-coupled two-nucleon wave functions, the matrix element for each $V(k)$ can be calculated from matrix element V:

$$\langle (ab), LS; JM|V(k)|(cd), L'S'; JM\rangle = (2k+1)(-1)^J \times \begin{Bmatrix} L & S & J \\ S' & L' & k \end{Bmatrix} \sum_{J'} (-1)^{J'}(2J'+1) \begin{Bmatrix} L & S & J' \\ S' & L' & k \end{Bmatrix} \times \langle (ab), LS; J'M|V|(cd), L'S'; J'M\rangle, \tag{6}$$

where a is shorthand notation for the set of quantum numbers n_a and l_a.

III. RESULTS AND DISCUSSION

A. Proton single-particle energy gaps

1. Sc and F isotopes

The ESPEs of proton orbitals in Sc and F isotopes are shown in Fig. 1. For Sc isotopes, it can be inferred that as neutrons occupy $\nu 0f$ orbitals, the energy gap between π-$0f_{7/2}$ and π-$0p$ orbitals enhances. Whereas, the same energy gap reduces when neutrons occupy $\nu 0p$ orbitals. The large energy gap between $\pi 0f_{7/2}$ and $\pi 1p_{3/2}$ orbitals at $N = 28$ is a conventional picture of the $Z = 28$ shell gap. While, the significant reduction in its strength at $N = 34$ points to its disappearance for ^{55}Sc. The energy gap between spin-orbital partners, i.e., between $\pi 0f_{7/2}$ and $\pi 0f_{5/2}$ orbitals, is nearly constant in Sc isotopes which indicates that the splitting of spin-orbital partners does not strongly depend on the NN interaction.

In F isotopes, as neutrons occupy ν-$0d$ orbitals, the energy between π-$0d_{5/2}$ and π-$1s_{1/2}$ orbitals increases. Whereas, this gap reduces when neutrons occupy the ν-$1s_{1/2}$ orbital. In case of proton spin-orbital partners, $\pi 0d_{5/2}$ and $\pi 0d_{3/2}$, the energy gap remains nearly constant as seen in Sc isotopes.

In Tables I and II, we summarize the contribution of proton-neutron central, spin-orbit, and tensor forces in the evolution of proton single-particle gaps in Sc and F isotopes, respectively. It is apparent from Eq. (3) that all proton orbitals have the same strength of the neutron-neutron interaction, thus, it does not contribute to germane proton single-particle energy gaps. Therefore, it is not considered in the discussion. Further, to make the discussion simple, the splitting between proton orbitals in Tables I and II is represented as the difference of only two J-averaged proton-neutron matrix elements at a time, and the reported numerical values are with respect to mass $A = 42$ for Sc isotopes and $A = 18$ for F isotopes. For any other mass A, new values can be obtained using corresponding mass correction factors mentioned earlier.

It can be followed from Table I that when neutrons occupy $\nu 0f$ orbitals, the central force predominantly contributes to enhance $\pi 1p_{3/2}$-$\pi 0f_{7/2}$ and $\pi 1p_{1/2}$-$\pi 0f_{7/2}$ energy gaps. The contribution of the central force to these energy gaps also

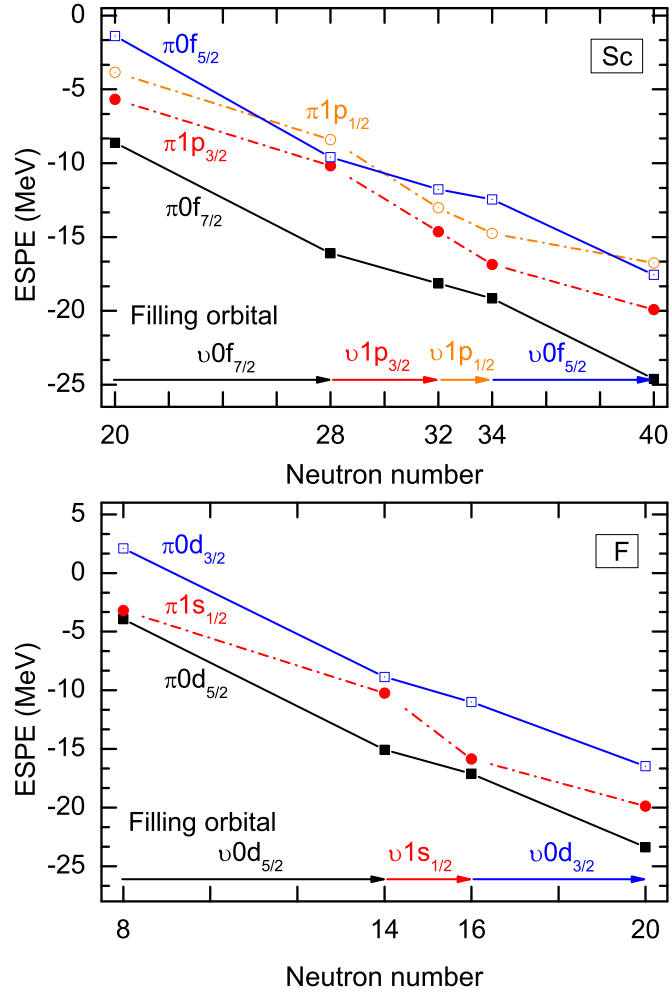

FIG. 1. ESPEs of π-$0f1p$ orbitals in Sc isotopes (upper panel) and π-$0d1s$ orbitals in F isotopes (lower panel).

remains dominant when neutrons occupy $\nu 1p$ orbitals, but, it acts with the opposite effect, which reduces the gaps. It is worth mentioning here that when the $\nu 1p_{1/2}$ orbital is occupied by neutrons, the contribution of the tensor force to the $\pi 1p_{1/2}$-$\pi 0f_{7/2}$ energy gap notably increases due to its characteristic nature [22] which aids to enhance the gap. However, this effect is negated by the central force which has nearly twice the strength of the tensor force with opposite nature. As a result, $\pi 1p_{1/2}$-$\pi 0f_{7/2}$ energy gap reduces. Further, it can be noted that the contribution of the central force is nearly same in the enhancement of the $\pi 1p$-$\pi 0f_{7/2}$ energy gaps from $N = 20$ to 28, and from 34 to 40, and also in the reduction of the same energy gaps from $N = 28$ to 32, and from 32 to 34. Such uniformity in the contribution of central force manifests that it possesses strong-orbital node (nl) and weak-spin (j) dependency. The strong-orbital node dependency of central force is also reported in Ref. [40], where it has been proved using the spin-exchange zero range δ interaction. In the spin-orbital partners energy gap $\pi 0f_{5/2}$-$\pi 0f_{7/2}$, the contribution of the central force is small, because the germane proton-neutron matrix elements have the same orbital nodes. The contribution of the spin-orbit force in it is similar to the contribution of

TABLE I. The contribution of central, spin-orbit, and tensor forces of proton-neutron interaction to proton single-particle energy gaps $\pi 1p_{3/2}$-$\pi 0f_{7/2}$, $\pi 1p_{1/2}$-$\pi 0f_{7/2}$, and $\pi 0f_{5/2}$-$\pi 0f_{7/2}$ in Sc isotopes. These results are with respect to mass number $A = 42$. See text for details. All values are given in MeV.

Energy gap		$\pi 1p_{3/2}$-$\pi 0f_{7/2}$		
Fillingorbital	$\nu 0f_{7/2}$ $N = 20 \to 28$	$\nu 0f_{5/2}$ $N = 34 \to 40$	$\nu 1p_{3/2}$ $N = 28 \to 32$	$\nu 1p_{1/2}$ $N = 32 \to 34$
Centroids	$\bar{V}^{\pi\nu}_{1p_{3/2}0f_{7/2}} - \bar{V}^{\pi\nu}_{0f_{7/2}0f_{7/2}}$	$\bar{V}^{\pi\nu}_{1p_{3/2}0f_{5/2}} - \bar{V}^{\pi\nu}_{0f_{7/2}0f_{5/2}}$	$\bar{V}^{\pi\nu}_{1p_{3/2}1p_{3/2}} - \bar{V}^{\pi\nu}_{0f_{7/2}1p_{3/2}}$	$\bar{V}^{\pi\nu}_{1p_{3/2}1p_{1/2}} - \bar{V}^{\pi\nu}_{0f_{7/2}1p_{1/2}}$
Central	0.478	0.416	−0.670	−0.617
Spin-orbit	−0.040	−0.037	−0.018	0.030
Tensor	−0.049	0.066	0.064	−0.127
Total	0.389	0.445	−0.624	−0.714
Energy gap		$\pi 1p_{1/2}$-$\pi 0f_{7/2}$		
Filling orbital	$\nu 0f_{7/2}$ $N = 20 \to 28$	$\nu 0f_{5/2}$ $N = 34 \to 40$	$\nu 1p_{3/2}$ $N = 28 \to 32$	$\nu 1p_{1/2}$ $N = 32 \to 34$
Centroids	$\bar{V}^{\pi\nu}_{1p_{1/2}0f_{7/2}} - \bar{V}^{\pi\nu}_{0f_{7/2}0f_{7/2}}$	$\bar{V}^{\pi\nu}_{1p_{1/2}0f_{5/2}} - \bar{V}^{\pi\nu}_{0f_{7/2}0f_{5/2}}$	$\bar{V}^{\pi\nu}_{1p_{1/2}1p_{3/2}} - \bar{V}^{\pi\nu}_{0f_{7/2}1p_{3/2}}$	$\bar{V}^{\pi\nu}_{1p_{1/2}1p_{1/2}} - \bar{V}^{\pi\nu}_{0f_{7/2}1p_{1/2}}$
Central	0.470	0.426	−0.624	−0.708
Spin-orbit	0.021	0.067	0.091	−0.061
Tensor	−0.110	0.147	−0.188	0.375
Total	0.381	0.640	−0.721	−0.394
Energy gap		$\pi 0f_{5/2}$-$\pi 0f_{7/2}$		
Filling orbital	$\nu 0f_{7/2}$ $N = 20 \to 28$	$\nu 0f_{5/2}$ $N = 34 \to 40$	$\nu 1p_{3/2}$ $N = 28 \to 32$	$\nu 1p_{1/2}$ $N = 32 \to 34$
Centroids	$\bar{V}^{\pi\nu}_{0f_{5/2}0f_{7/2}} - \bar{V}^{\pi\nu}_{0f_{7/2}0f_{7/2}}$	$\bar{V}^{\pi\nu}_{0f_{5/2}0f_{5/2}} - \bar{V}^{\pi\nu}_{0f_{7/2}0f_{5/2}}$	$\bar{V}^{\pi\nu}_{0f_{5/2}1p_{3/2}} - \bar{V}^{\pi\nu}_{0f_{7/2}1p_{3/2}}$	$\bar{V}^{\pi\nu}_{0f_{5/2}1p_{1/2}} - \bar{V}^{\pi\nu}_{0f_{7/2}1p_{1/2}}$
Central	0.056	−0.074	−0.006	0.012
Spin-orbit	0.011	−0.081	0.014	0.057
Tensor	−0.163	0.217	−0.047	0.094
Total	−0.096	0.062	−0.039	0.163

the central force. The tensor force relatively contributes large, but not large enough to produce a notable variation. Thus, the energy gap between spin-orbital partners remains nearly constant in Sc isotopes.

In F isotopes, the variation in $\pi 1s_{1/2}$-$\pi 0d_{5/2}$ energy gap mainly depends on central force, see Table II. It predominantly enhances and reduces this energy gap as neutrons occupy ν-$0d$ and ν-$1s_{1/2}$ orbitals, respectively. Furthermore,

TABLE II. The contribution of central, spin-orbit, and tensor forces of proton-neutron interaction to proton single-particle energy gaps $\pi 1s_{1/2}$-$\pi 0d_{5/2}$ and $\pi 0d_{3/2}$-$\pi 0d_{5/2}$ in F isotopes. These results are with respect to mass number $A = 18$. All values are given in MeV.

Energy gap		$\pi 1s_{1/2}$-$\pi 0d_{5/2}$	
Fillingorbital	$\nu 0d_{5/2}$ $N = 8 \to 14$	$\nu 0d_{3/2}$ $N = 16 \to 20$	$\nu 1s_{1/2}$ $N = 14 \to 16$
Centroids	$\bar{V}^{\pi\nu}_{1s_{1/2}0d_{5/2}} - \bar{V}^{\pi\nu}_{0d_{5/2}0d_{5/2}}$	$\bar{V}^{\pi\nu}_{1s_{1/2}0d_{3/2}} - \bar{V}^{\pi\nu}_{0d_{5/2}0d_{3/2}}$	$\bar{V}^{\pi\nu}_{1s_{1/2}1s_{1/2}} - \bar{V}^{\pi\nu}_{0d_{5/2}1s_{1/2}}$
Central	0.680	0.634	−1.902
Spin-orbit	0.189	−0.172	−0.021
Tensor	−0.129	0.194	0.000
Total	0.740	0.656	−1.923
Energy gap		$\pi 0d_{3/2}$-$\pi 0d_{5/2}$	
Filling orbital	$\nu 0d_{5/2}$ $N = 8 \to 14$	$\nu 0d_{3/2}$ $N = 16 \to 20$	$\nu 1s_{1/2}$ $N = 14 \to 16$
Centroids	$\bar{V}^{\pi\nu}_{0d_{3/2}0d_{5/2}} - \bar{V}^{\pi\nu}_{0d_{5/2}0d_{5/2}}$	$\bar{V}^{\pi\nu}_{0d_{3/2}0d_{3/2}} - \bar{V}^{\pi\nu}_{0d_{5/2}0d_{3/2}}$	$\bar{V}^{\pi\nu}_{0d_{3/2}1s_{1/2}} - \bar{V}^{\pi\nu}_{0d_{5/2}1s_{1/2}}$
Central	0.046	−0.069	0.000
Spin-orbit	0.307	−0.183	−0.053
Tensor	−0.323	0.485	0.000
Total	0.030	0.230	−0.053

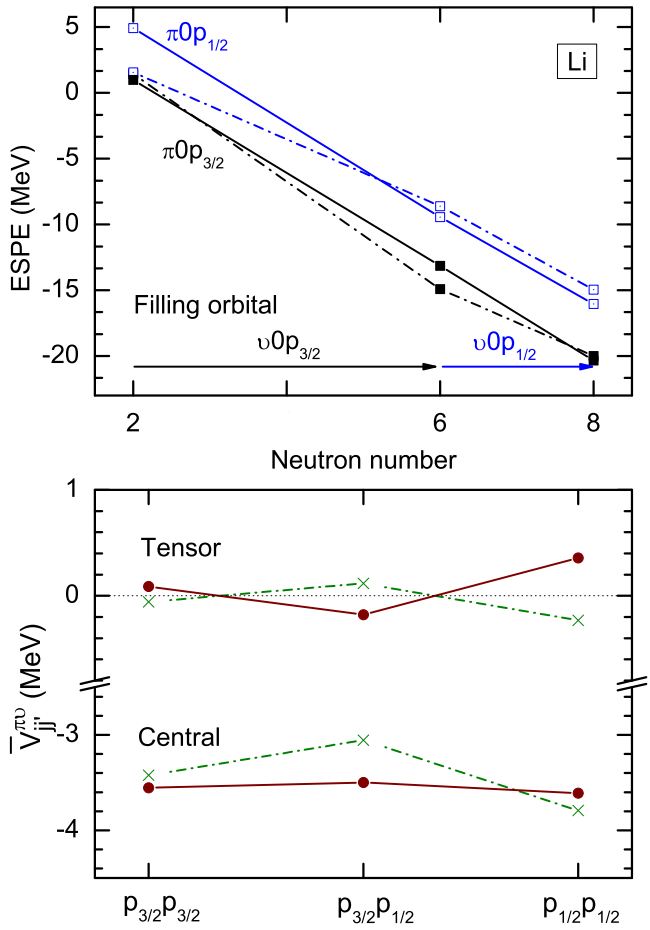

FIG. 2. Upper panel: ESPEs of π-0p orbitals in Li isotopes. Lower panel: J-averaged proton-neutron central and tensor force matrix elements in 0p shell. The dot-dash and solid line are used for CK(8-16)and CKHeN interactions, respectively.

the contribution of central force in the $\pi 1s_{1/2}$-$\pi 0d_{5/2}$ energy gap is nearly the same when ν-0d orbitals are occupied by neutrons. Thus, it confirms that the proton-neutron central force in the 0d1s shell also possesses strong-orbital node and weak-spin dependency. The effect of this property of central force can also be seen for the $\pi 0d_{3/2}$-$\pi 0d_{5/2}$ energy gap where it has a small contribution. Further, in the $\pi 0d_{3/2}$-$\pi 0d_{5/2}$ energy gap, noncentral forces contribute with notable strength when ν-0d orbitals are occupied by neutrons, but they contribute destructively with respect to each other. In the same energy gap, the individual contribution of noncentral forces is insignificant when the ν-$1s_{1/2}$ orbital is occupied by neutrons. Thus, the single-particle energy gap between $\pi 0d_{3/2}$ and $\pi 0d_{5/2}$ orbitals remains nearly constant in F isotopes.

2. Li isotopes

The ESPEs of π-0p orbitals are shown in Fig. 2. The calculations are first performed with the CK(8-16) interaction [48] and it is observed that the energy gap between spin-orbital partners, $\pi 0p_{3/2}$ and $\pi 0p_{1/2}$, increases when neutrons occupy the $\nu 0p_{3/2}$ orbital. However, this energy gap should remain nearly constant as noted in Sc and F isotopes. This unusual variation may be due to a lack of common features in the proton-neutron central and tensor forces of the CK(8-16) interaction. Its proton-neutron central force does not possess weak-spin dependency, and its tensor force does not have the regular nature [22], see Fig. 2. In order to ameliorate these discrepancies, we have constructed a hybrid interaction. In the beginning, the interaction consists of single-particle energies of 0p orbitals and $T = 1$ two-body matrix elements of the interaction developed in Ref. [49], and $T = 0$ two-body matrix elements of the CK(8-16) interaction. The two-body matrix elements of this integrated interaction, mainly the diagonal matrix elements, have been modified in such a way that the resultant interaction could predict single-particle properties in Li isotopes, and its proton-neutron central and tensor forces gain their common features. Note that the spin-tensor decomposition has been performed at each step of modification to check the properties of central and tensor forces. The final interaction named CKHeN, and its proton-neutron central and tensor forces are shown in Fig. 2. It can be seen that in the CKHeN interaction, the proton-neutron central force is obtained with good weak-spin dependency, and proton-neutron tensor force is obtained with its characteristic properties. The ESPEs of $\pi 0p$ orbitals calculated using the CKHeN interaction are also shown in Fig. 2, and it can be seen that the energy gap between $\pi 0p_{3/2}$ and $\pi 0p_{1/2}$ orbitals stays nearly constant in Li isotopes.

TABLE III. Contribution of central, spin-orbit and tensor forces of proton-neutron interaction of CKHeN interaction to proton single particle energy gap $\pi 0p_{1/2}$-$\pi 0p_{3/2}$ in Li isotopes. All values are given in MeV.

Energy gap	$\pi 0p_{1/2} - \pi 0p_{3/2}$	
Filling orbital	$\nu 0p_{3/2}$ $N = 2 \rightarrow 6$	$\nu 0p_{1/2}$ $N = 6 \rightarrow 8$
Centroids	$\bar{V}^{\pi\nu}_{0p_{1/2}0p_{3/2}} - \bar{V}^{\pi\nu}_{0p_{3/2}0p_{3/2}}$	$\bar{V}^{\pi\nu}_{0p_{1/2}0p_{1/2}} - \bar{V}^{\pi\nu}_{0p_{3/2}0p_{1/2}}$
Central	0.056	−0.113
Spin-orbit	0.154	−0.127
Tensor	−0.268	0.537
Total	−0.058	0.297

The contribution of different components of the proton-neutron interaction to the $\pi 0p_{1/2}$-$\pi 0p_{3/2}$ energy gap is given in Table III. As can be seen from this table, the contribution of the central force is consistent with its strong-orbital node and weak-spin dependency property. When neutrons occupy $\nu 0p_{3/2}$ and $\nu 0p_{1/2}$ orbitals, the contribution of the spin-orbit force is greater and comparable with the contribution of a central force, respectively. The contribution of the tensor force is relatively large. However, its effect is reduced by the spin-orbital force, and also by the central force when neutrons occupy the $0p_{1/2}$ orbital. Thus, the $\pi 0p_{1/2}$-$\pi 0p_{3/2}$ energy gap remains nearly constant in Li isotopes.

B. Level structure and proton single-particle strength

To better understand the influence of proton single-particle energy gaps on the level structure of Sc, F, and Li isotopes,

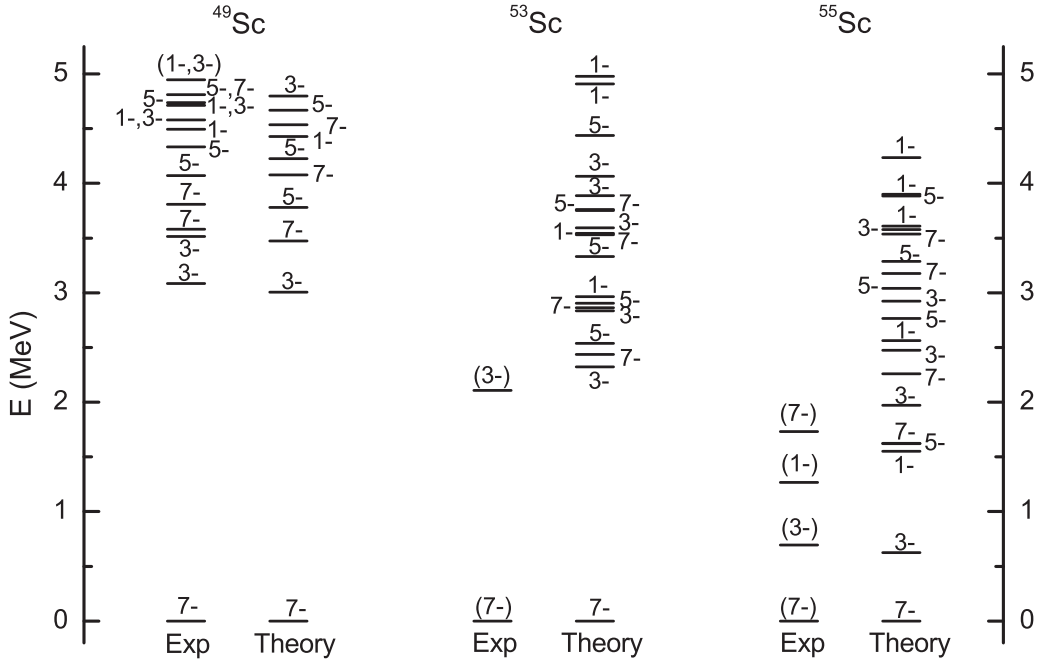

FIG. 3. Level structure of ^{49,53,55}Sc. Only negative parity states $\frac{7}{2}^-$, $\frac{3}{2}^-$, $\frac{1}{2}^-$, and $\frac{5}{2}^-$ are shown. All states are denoted by $2J$.

we have carried out large-scale shell-model calculations using the shell model code NUSHELLX@MSU [50]. In the present work, the calculations have been performed for ^{49,53,55}Sc, ^{23,25}F, and ^{9}Li isotopes. These isotopes are adjacent to $A-1$, $Z-1$ magic/semimagic nuclei; therefore, the effect of proton single-particle energy gaps on their level structure can be determined easily. We have calculated the level structure of those nuclei, and the proton-transfer spectroscopic factors C^2S values for their few specific states.

1. ^{49,53,55}Sc *isotopes*

Figure 3 shows theoretical and experimental level structure of ^{49,53,55}Sc isotopes [34–36]. The agreement between theory and experiment for these isotopes is satisfactory. For instance, theory fairly reproduces $\frac{3}{2}^-_1$ state of these isotopes, and also the decrease in its excitation energy from ^{49}Sc to ^{55}Sc. Further, theory reasonably reproduces other low-lying states of ^{55}Sc.

The C^2S values are calculated for $\frac{7}{2}^-$, $\frac{5}{2}^-$, $\frac{3}{2}^-$, and $\frac{1}{2}^-$ states of ^{49,53,55}Sc with respect to ^{48,52,54}Ca, respectively. Here, the transfer of a proton to Ca isotopes manifests that the transferred proton may occupy either of $\pi-0f_{7/2}$, $-0f_{5/2}$, $-1p_{3/2}$, and $-1p_{1/2}$ orbitals which are associated with $\frac{7}{2}^-$, $\frac{5}{2}^-$, $\frac{3}{2}^-$, and $\frac{1}{2}^-$ states, respectively. Thus, the magnitude of C^2S clearly indicates the proton single-particle strength in these states. The theoretical C^2S values are shown in Fig. 4. The experimental C^2S values known for the ground state $\frac{7}{2}^-$ and excited state $\frac{3}{2}^-_1$ of ^{49}Sc [51] are also shown in Fig. 4. These theoretical and experimental C^2S values are found to be in good agreement. Further, the ground state $\frac{7}{2}^-$ of ^{49,53,55}Sc isotopes can be seen to contain approximately 90% of the total proton single-particle strength. In ^{49,53}Sc, the $\frac{3}{2}^-_1$ state contains a competent proton single-particle strength. Therefore, the high excitation energy of $\frac{3}{2}^-_1$ state of ^{49}Sc, and its decrease for ^{53}Sc in Fig. 3 can be understood as caused by an enhanced and reduced $\pi 0f_{7/2}$-$\pi 1p_{3/2}$ energy gap at $N=28$ and 32, respectively. In the case of the $\frac{3}{2}^-_1$ state of ^{55}Sc, the single-particle strength is small; hence, its low excitation energy is not related to a further decrease of the $\pi 0f_{7/2}$-$\pi 1p_{3/2}$ energy gap at $N=34$. This low excited state most likely originates from the transition of a neutron across the $N=34$ semimagic shell gap which probably gets weak for ^{55}Sc. The occupation numbers of $\pi 1p_{3/2}$, $\pi 1p_{1/2}$, and $\nu 0f_{5/2}$ orbitals for this state are 0.16, 1.06, and 1.07, respectively, which also support the diminution of the $N=34$ energy gap for ^{55}Sc. The $\frac{3}{2}^-$ state of ^{55}Sc, for which proton single-particle strength is sizable, is present around 2.5 MeV. The high excitation energy of this state may be caused by additional correlations developed from configuration mixing. For this state, the occupation numbers of $\pi 1p_{3/2}$, $\pi 1p_{1/2}$, and $\nu 0f_{5/2}$ orbitals are 0.46, 1.56, and 0.91, respectively. For $\frac{1}{2}^-$ and $\frac{5}{2}^-$ states of ^{49,53,55}Sc, single-particle strength is fragmented over a broad range of excitation energy; therefore, the effect of proton single-particle energy gaps on the excitation energies of these states could not be determined.

2. ^{23,25}F *isotopes*

The theoretical and experimental level spectra of ^{23,25}F [37–39] are shown in Fig. 5. The $\frac{1}{2}^+_1$ state of both isotopes and the decrease in its excitation energy from ^{23}F to ^{25}F are well reproduced by theory. Overall, theory fairly reproduces experimental level structure. For ^{23,25}F, C^2S values are calculated for $\frac{5}{2}^+$, $\frac{1}{2}^+$, and $\frac{3}{2}^+$ states with respect to ^{22,24}O, respectively. These values along with experimental values

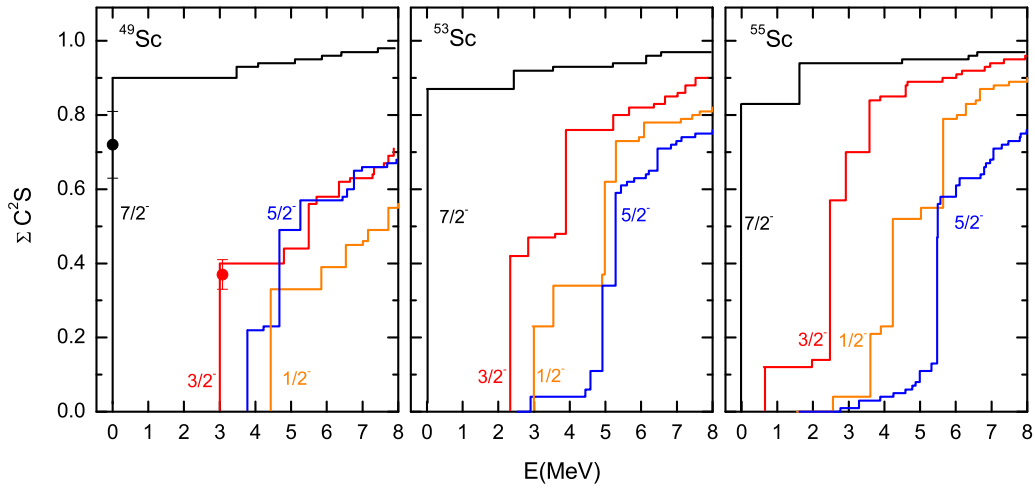

FIG. 4. Proton transfer spectroscopic factor C^2S for $\frac{7}{2}^-$ (black), $\frac{3}{2}^-$ (red), $\frac{1}{2}^-$ (orange), and $\frac{5}{2}^-$ (blue) states of ^{49,53,55}Sc isotopes.

of ^{23}F [37] are shown in Fig. 5. Within the limit of the reduction factor (∼0.5) as observed in nucleon transfer reactions [52,53], these theoretical values of ^{23}F are in reasonable agreement with experimental values. This reduction in spectroscopic factors is attributed to mixing with configurations beyond the $0d1s$ shell that is generated by short-range and tensor NN correlations [54].

Further, it can be followed from Fig. 5 that the $\frac{5}{2}^+$ ground state and $\frac{1}{2}^+_1$ excited state of ^{23,25}F contain significant single-particle strength. Thus, the high energy of the $\frac{1}{2}^+_1$ state of ^{23}F and relatively low energy of the $\frac{1}{2}^+_1$ state of ^{25}F can be apprehended as caused by an enhanced and reduced $\pi 1s_{1/2}$-$\pi 0d_{5/2}$ energy gap at $N = 14$ and 16, respectively. The $\frac{3}{2}^+_1$ state of ^{23}F also possesses marked single-particle strength; therefore, the high energy of this state can also be apprehended as caused by large $\pi 0d_{3/2}$-$\pi 0d_{5/2}$ energy gap present at $N = 14$. In ^{25}F, the $\frac{3}{2}^+_1$ state possesses trivial single-particle strength, therefore, this state is not associated with a large $\pi 0d_{3/2}$-$\pi 0d_{5/2}$ energy gap present at $N = 16$. For this state, the occupation numbers of $\pi 0d_{3/2}$, $\nu 1s_{1/2}$, and $\nu 0d_{3/2}$ orbitals in order are 0.13, 1.13, and 1.07 which connote that this state is mainly originated from the transition of a $\nu 1s_{1/2}$ neutron across a large $\nu 1s_{1/2}$-$\pi 0d_{3/2}$ energy gap present at $N = 16$ for semimagic nucleus ^{24}O [55]. The $\frac{3}{2}^+$ state of ^{25}F which has notable features of single-particle strength and the

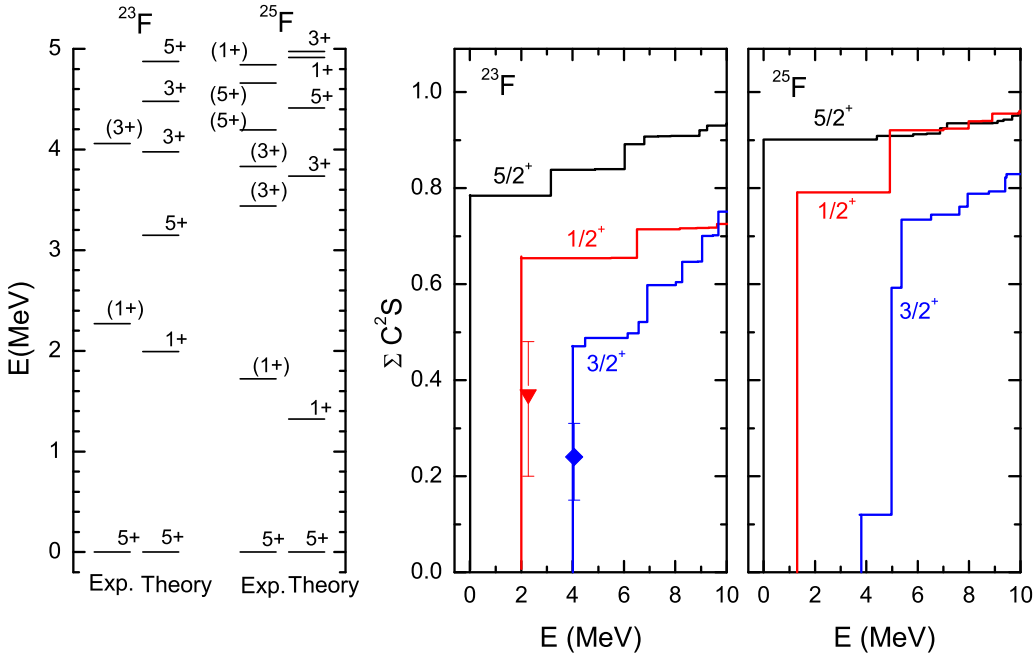

FIG. 5. Left: Level structure of ^{23,25}F. Only positive parity states $\frac{5}{2}^+$, $\frac{1}{2}^+$, and $\frac{3}{2}^+$ are shown. All states are shown by $2J$. Middle and right: Proton transfer spectroscopic factor C^{2}S for $\frac{5}{2}^+$ (black), $\frac{1}{2}^+$ (red), and $\frac{3}{2}^+$ (blue) states of ^{23,25}F.

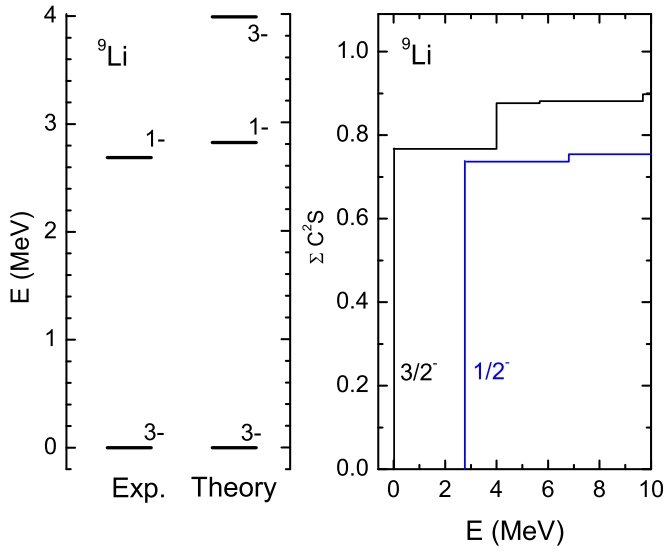

FIG. 6. Left: Level structure of ^{9}Li. Only negative parity states $\frac{3}{2}^-$ and $\frac{1}{2}^-$ are shown. All states are shown by $2J$. Right: Proton transfer spectroscopic factor C^2S for $\frac{3}{2}^-$ (black) and $\frac{1}{2}^-$ (blue) states of ^{9}Li.

$\pi 0d_{3/2}$-$\pi 0d_{5/2}$ energy gap is present around 5 MeV. For this state, the occupation numbers of $\pi 0d_{3/2}$, $\nu 1s_{1/2}$, and $\nu 0d_{3/2}$ orbitals are 0.49, 1.68, and 0.69, respectively.

3. ^{9}Li *isotope*

The shell model calculation for ^{9}Li is performed with the CKHeN interaction. Theoretical and experimental level structures [56] of it are shown in Fig. 6, and are found to be in good equivalence. The theoretical C^2S values of $\frac{3}{2}^-$ and $\frac{1}{2}^-$ states of ^{9}Li calculated with respect to ^{8}He are also shown in Fig. 6. It depicts that the ground state $\frac{3}{2}^-$ and first excited state $\frac{1}{2}^-$ contain nearly 75% of total proton single-particle strength. Therefore, the origin of the highly excited first $\frac{1}{2}^-$ state of ^{9}Li can be delineated as the transition of a proton from the $\pi 0p_{3/2}$ orbital to $\pi 0p_{1/2}$ orbital, where the single-particle energy gap between these orbitals remained constant when going from ^{5}Li to ^{9}Li.

IV. SUMMARY

In this work, the effect of proton-neutron interaction on the proton-shell structure of odd-A Sc, F, and Li isotopes is presented. The spin-tensor decomposition is shown to determine qualitatively the role played by different components of proton-neutron interaction in the evolution of proton shell structure within a shell. It is discerned that central force possesses strong-orbital node and weak-spin dependency. It plays an important role to enhance/reduce proton $\pi 1p$-$\pi 0f_{7/2}$ energy gaps in Sc isotopes, and the $\pi 1s_{1/2}$-$\pi 0d_{5/2}$ energy gap in F isotopes. The energy gap between spin-orbitals partners, i.e., $\pi 0f_{5/2,7/2}$ in Sc isotopes, $\pi 0d_{3/2,5/2}$ in F isotopes, and $\pi 0p_{1/2,3/2}$ in Li isotopes, stays nearly constant. The contribution of central force is small in spin-orbital partners energy gaps since the germane proton-neutron matrix elements have the same orbital nodes. Further, the contribution of spin-orbit and tensor forces is found to be small in spin-orbital partners energy gap for Sc isotopes. While this contribution is substantial in F and Li isotopes. These noncentral forces interfere destructively with each other in F and Li isotopes.

The integrated effect of proton single-particle energy gaps and proton single-particle strength in constructing the level structure of ^{49,53,55}Sc, ^{23,25}F, and ^{9}Li isotopes are also presented in this work. It is particularly recognized that the low-energy of the $\frac{3}{2}^-_1$ state of ^{55}Sc is caused by the weakening of the $N = 34$ semimagic gap instead of a sizable decrease of the $Z = 28$ magic shell gap. Furthermore, the high-energy of the $\frac{1}{2}^+_1$ state of ^{23}F is attributed to the increase of the energy gap between $\pi 1s_{1/2}$ and $\pi 0d_{5/2}$ orbitals at $N = 14$, and the high energy of the $\frac{1}{2}^-_1$ state of ^{9}Li is attributed to the large energy gap between $\pi 0p_{1/2}$ and $\pi 0p_{3/2}$ orbitals which remained constant from ^{5}Li to ^{9}Li.

ACKNOWLEDGMENTS

P.K. thanks N. A. Smirnova, P. K. Rath, and S. K. Ghorui for the scientific discussions, and their continuous interest in this work. He also thanks R. G. Pillay and Arshiya Sood for helpful suggestions in writing the manuscript.

[1] M. G. Mayer, Phys. Rev. **75**, 1969 (1949).
[2] A. Ozawa, T. Kobayashi, T. Suzuki, K. Yoshida, and I. Tanihata, Phys. Rev. Lett. **84**, 5493 (2000).
[3] O. Sorlin *et al.*, Prog Part, Nucl. Phys. **61**, 602 (2008).
[4] E. Becheva *et al.*, Phys. Rev. Lett. **96**, 012501 (2006).
[5] K. Tshoo, Y. Satou, H. Bhang, S. Choi, T. Nakamura, Y. Kondo, S. Deguchi, Y. Kawada, N. Kobayashi, Y. Nakayama, K. N. Tanaka, N. Tanaka, N. Aoi, M. Ishihara, T. Motobayashi, H. Otsu, H. Sakurai, S. Takeuchi, Y. Togano, K. Yoneda, Z. H. Li, F. Delaunay, J. Gibelin, F. M. Marques, N. A. Orr, T. Honda, M. Matsushita, T. Kobayashi, Y. Miyashita, T. Sumikama, K. Yoshinaga, S. Shimoura, D. Sohler, T. Zheng, and Z. X. Cao, Phys. Rev. Lett. **109**, 022501 (2012).
[6] F. Wienholtz *et al.*, Nature **498**, 346 (2013).
[7] D. Steppenbeck *et al.*, Nature **502**, 207 (2013).
[8] T. Al Kalanee *et al.*, Phys. Rev. C **88**, 034301 (2013).
[9] Yu. Aksyutina *et al.*, Phys. Lett. B **666**, 430 (2008).
[10] H. Simon *et al.*, Phys. Rev. Lett. **83**, 496 (1999).
[11] S. D. Pain *et al.*, Phys. Rev. Lett. **96**, 032502 (2006).
[12] Y. Kondo *et al.*, Phys. Rev. Lett. **116**, 102503 (2016).
[13] P. Doornenbal *et al.*, Phys. Rev. C **95**, 041301(R) (2017).
[14] S. M. Brown *et al.*, Phys. Rev. C **85**, 011302(R) (2012).
[15] H. N. Liu *et al.*, Phys. Lett. B **767**, 58 (2017).
[16] M. Petri *et al.*, Phys. Lett. B **748**, 173 (2015).
[17] B. V. Pritychenko, T. Glasmacher, B. A. Brown, P. D. Cottle, R. W. Ibbotson, K. W. Kemper, L. A. Riley, and H. Scheit, Phys. Rev. C **63**, 011305(R) (2000).
[18] T. Motobayashi *et al.*, Phys. Lett. B **346**, 9 (1995).

[19] P. Doornenbal *et al.*, Phys. Rev. Lett. **111**, 212502 (2013).
[20] S. Takeuchi *et al.*, Phys. Rev. Lett. **109**, 182501 (2012).
[21] K. T. Flanagan *et al.*, Phys. Rev. Lett. **103**, 142501 (2009).
[22] T. Otsuka, T. Suzuki, R. Fujimoto, H. Grawe, and Y. Akaishi, Phys. Rev. Lett. **95**, 232502 (2005).
[23] T. Otsuka, T. Suzuki, M. Honma, Y. Utsuno, N. Tsunoda, K. Tsukiyama, and M. Hjorth-Jensen, Phys. Rev. Lett. **104**, 012501 (2010).
[24] T. Otsuka, T. Matsuo, and D. Abe, Phys. Rev. Lett. **97**, 162501 (2006).
[25] M. Grasso, Phys. Rev. C **89**, 034316 (2014).
[26] E. Yäksel, N. VanGiai, E. Khan, and K. Bozkurt, Phys. Rev. C **89**, 064322 (2014).
[27] G. Colò *et al.*, Phys. Lett. B **646**, 227 (2007).
[28] N. Tsunoda, T. Otsuka, K. Tsukiyama, and M. Hjorth-Jensen, Phys. Rev. C **84**, 044322 (2011).
[29] N. A. Smirnova *et al.*, Phys. Lett. B **686**, 109 (2010); Phys. Rev. C **86**, 034314 (2012).
[30] A. Umeya and K. Muto, Phys. Rev. C **69**, 024306 (2004); A. Umeya *et al.*, *ibid.* **74**, 034330 (2006); Nucl. Phys. A **955**, 194 (2016).
[31] M. W. Kirson, Phys. Lett. B **47**, 110 (1973).
[32] K. Klingenbeck *et al.*, Phys. Rev. C **15**, 1483 (1977).
[33] X. B. Wang *et al.*, J. Phys. G: Nucl. Part. Phys. **42**, 125101 (2015).
[34] S. Bhattacharyya *et al.*, Phys. Rev. C **79**, 014313 (2009).
[35] S. McDaniel *et al.*, Phys. Rev. C **81**, 024301 (2010).
[36] D. Steppenbeck *et al.*, Phys. Rev. C **96**, 064310 (2017).
[37] S. Michimasa *et al.*, Phys. Lett. B **638**, 146 (2006); Nucl. Phys. A **787**, 569 (2007).
[38] Z. Vajta *et al.*, Phys. Rev. C **89**, 054323 (2014).
[39] M. Vandebrouck *et al.* (R3B collaboration), Phys. Rev. C **96**, 054305 (2017).
[40] N. A. Smirnova, A. De Maesschalck, A. Van Dyck, and K. Heyde, Phys. Rev. C **69**, 044306 (2004).
[41] P. Kumar *et al.*, Nucl. Phys. A **983**, 210 (2019).
[42] P. J. Brussaard and P. W. M. Glaudemans, *Shell Model Applications in Nuclear Spectroscopy* (North-Holland Publishing, Amsterdam, 1977).
[43] A. Poves *et al.*, Phys. Rep. **70**, 235 (1981).
[44] A. P. Zuker, Nucl. Phys. A **576**, 65 (1994).
[45] M. Dufour and A. P. Zuker, Phys. Rev. C **54**, 1641 (1996).
[46] M. Honma *et al.*, RIKEN Accel. Prog. Rep. **41**, 32 (2008).
[47] B. A. Brown and W. A. Richter, Phys. Rev. C **74**, 034315 (2006).
[48] S. Cohen *et al.*, Nucl. Phys. A **73**, 1 (1965).
[49] J. Stevenson *et al.*, Phys. Rev. C **37**, 2220 (1988).
[50] B. A. Brown *et al.*, Nucl. Data Sheets **120**, 115 (2014).
[51] J. W. Watson *et al.*, Phys. Rev. C **40**, 570 (1989).
[52] A. Signoracci and B. A. Brown, Phys. Rev. C **75**, 024303 (2007).
[53] J. Lee, J. A. Tostevin, B. A. Brown, F. Delaunay, W. G. Lynch, M. J. Saelim, and M. B. Tsang, Phys. Rev. C **73**, 044608 (2006).
[54] W. H. Dickhoff *et al.*, Prog. Part. Nucl. Phys. **52**, 377 (2004).
[55] B. A. Brown, Int. J. Mod. Phys. E **26**, 1740003 (2017).
[56] E. Tengborn *et al.*, Phys. Rev. C **84**, 064616 (2011).